2.5-km Low-Temperature Multiple-Reflection Cell

D. Horn and G. C. Pimentel

A low-temperature multiple-pass White cell is described which can be operated at any temperature between 120 K and room temperature. The path length can be varied from 60 m up to 2540 m in 80-m steps. The four-row multiple reflection system, a modified White arrangement, is enclosed in an aluminum dewar and can be focused externally while cold. An approximate expression for the astigmatic image distortion in a cell of the described type is derived.

Introduction

In order to interpret quantitatively the infrared spectra of the Martian atmosphere as obtained by the IRS spectrometers of Mariner VI and Mariner VII,[1] it was necessary to study the dependence of the absorption of CO_2, H_2O, CO, and other gases on pressure, temperature, and amount under conditions that simulate Martian conditions. In particular, there was a need for absorption data of large CO_2 samples and trace quantities of other gases in a temperature range between 150 K and 300 K at pressures of a few millibars. Multiple traversal cells operating at low temperatures have been described[2-6] in which cooling is achieved with a refrigerant like liquid nitrogen, liquid hydrogen, liquid argon, or dry ice. These cells, therefore, were conveniently operated at fixed temperatures determined by the convenient coolants. The longest path length was obtained by Blickensderfer and co-workers with 320 m. The cell described by McKeller *et al.*[7] could be used up to 165 m and allowed a temperature control within a small range, depending on the selected refrigerant and limited by a maximum operating pressure of the *cryogenerator* of 30 bar.

In the following we will describe the design and the operation of a multiple reflection cell continuously controllable in temperature within a range of 120 K to 300 K and with a maximum path length of 2540 m.

Both authors were with the Chemistry Department, University of California, Berkeley, California 94720, when this work was done; D. Horn is now with Badische Anilin- und Soda-Fabrik AG, Ludwigshafen, Germany.

Received 8 March 1971.

Dewar

Design

The cell consists of a four-row multiple reflection system enclosed in an aluminum dewar assembly. The aluminum alloy 5086 was selected for the construction of the dewar assembly to meet the stringent requirements for maintenance of high vacuum, for good heat transfer, and for high corrosion resistance. (The construction and welding of the dewar assembly were performed by Allied Engineering and Production Corp., Alameda, California.) Figure 1 shows the dewar in cross section. It consists of an inner chamber (63.5-cm i.d.), which is the sample compartment, and an outer vessel (79-cm i.d.), which serves as a vacuum tank for thermal insulation of the inner chamber. The over-all external length is 11 m. There are 56 cooling channels welded to the skin of the inner vessel to provide temperature uniformity with maximum fluctuations of less than 0.2°C over the entire length of the dewar. Both vessels are interlocked at the center (Fig. 1) by means of a SS304 bellows for low heat conductance. Thus both halves of the inner tank can ride freely on eight nylon rollers to allow for extension and contraction with changing temperature. To minimize convection currents in the gas sample, the orifice of the 30.5-cm elbow can be covered with a baffle as shown in Fig. 1. The baffle temperature is controlled with a separate coolant circuit and the baffle can be opened externally during pumping. All flanges of the inner chamber are sealed with Teflon-coated metal seals for cryogenics. The seals of the large-diameter flanges, e.g., the pumpout port and the endplates of the tank, are Teflon-coated metal O rings (United Aircraft, Inc.). All small-diameter feedthrough flanges are sealed with Teflon-coated metal V seals (Haskel Engineering).

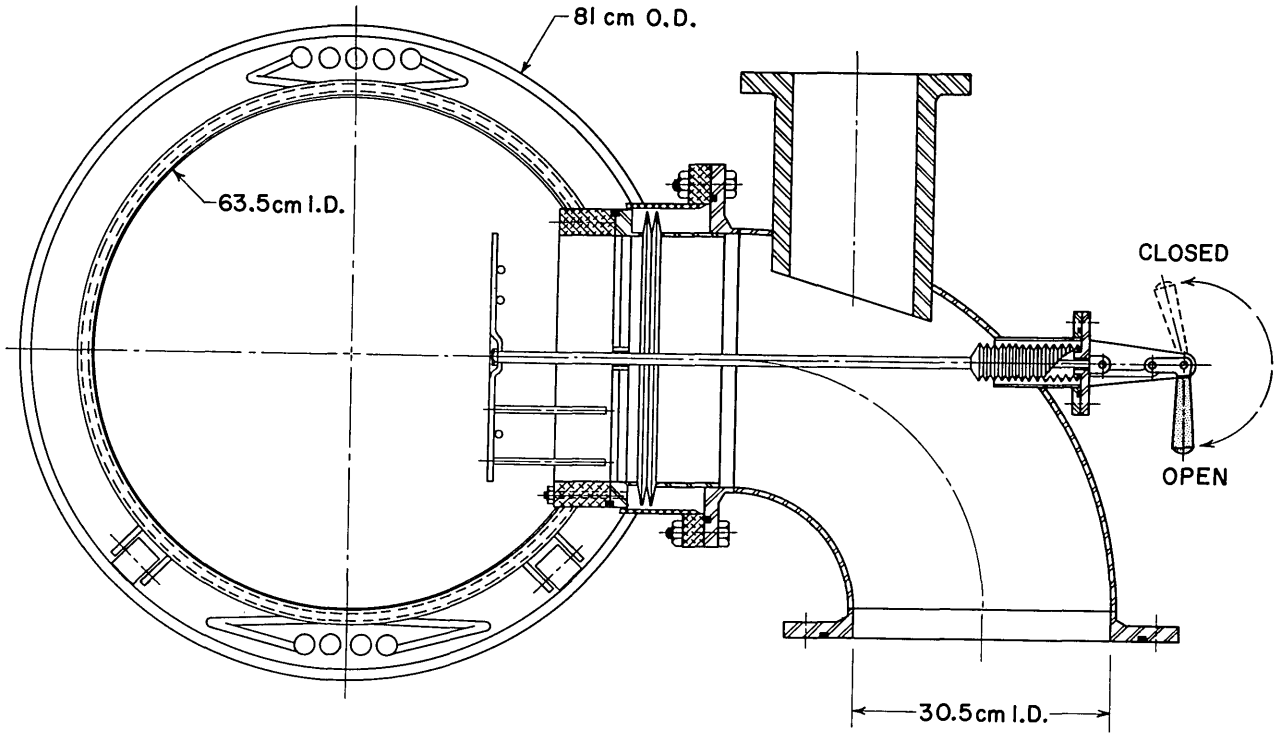

Fig. 1. Cross section of the dewar assembly.

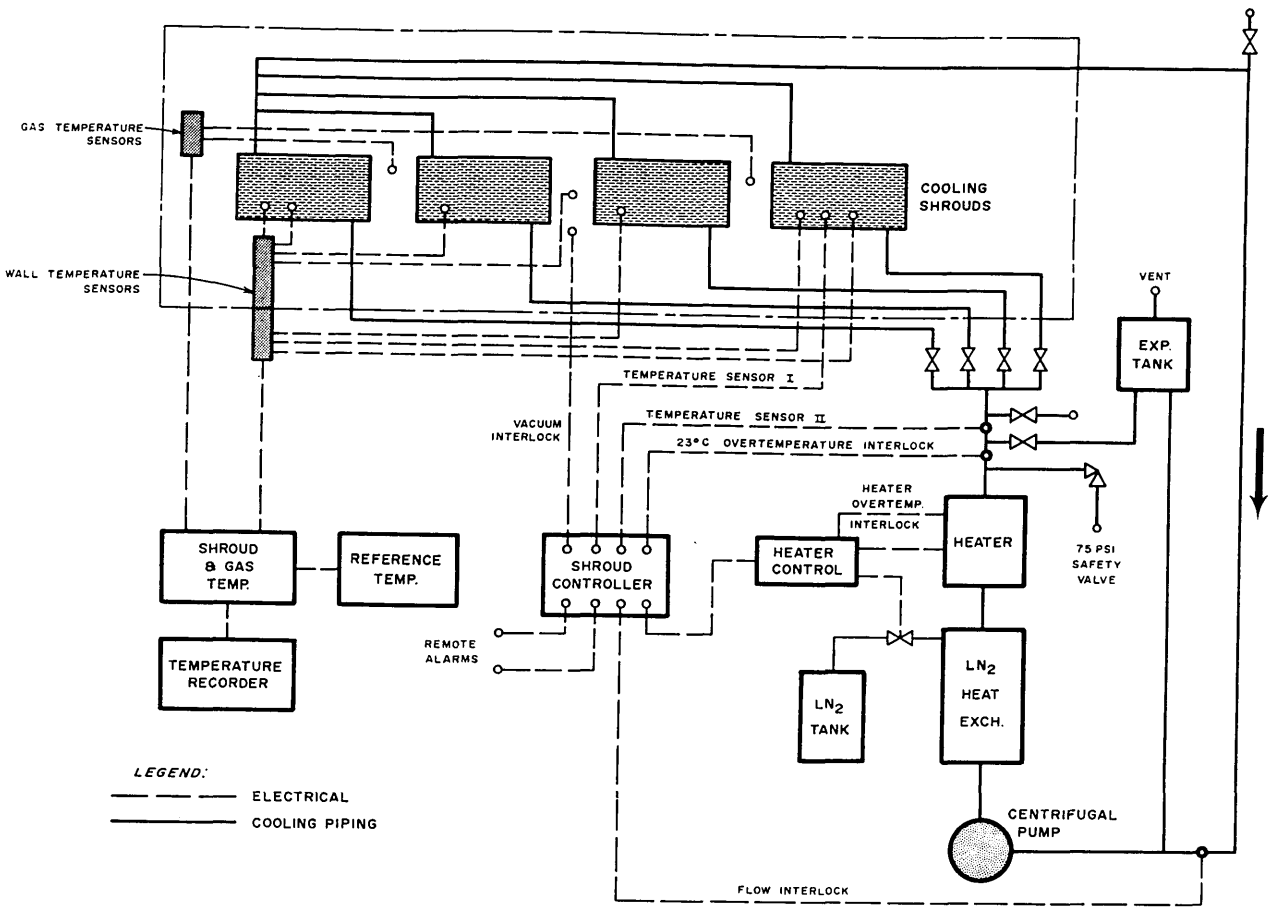

Fig. 2. Cryogenic system, schematic.

Pumping System

A two-stage Roots blower system is used for reducing the pressure from 1 atm to below 10^{-3} Torr in both inner and outer vessels. It consists of a Heraeus RG-350 mechanical blower backed by a Kinney KMBD-1600/KT-150 booster vacuum system. The time for evacuation from atmospheric pressure to 2×10^{-3} Torr is typically 15–20 min. This roughing system ultimately can reach about 3×10^{-5} Torr. For further evacuation of the inner chamber an Ultek–Perkin-Elmer ion pump system (RCS, 200 liters/sec) with titanium sublimation and cryopanel is connected to the 30.5-cm elbow. This system further evacuates the inner vessel to 3×10^{-7} Torr within 4–5 h. After roughing of the outer vacuum jacket with the blower system, a vacuum in the low 10^{-5} Torr range is maintained by means of a 15-cm VHS NRC oil diffusion pump. This pressure range is sufficiently low to limit the heat transfer essentially to radiation losses.

Cryogenic System

Coolant Circulation System

Figure 2 shows schematically the cooling jacket supply system. The cooling channel assembly already described is partitioned into four independent sections, and each channel is individually fed and discharged by a manifold. The coolant, a 1:4 mixture of isohexane and isopentane, is circulated by a centrifugal pump and passes outside the chamber through a heat exchanger and a heater assembly. This coolant mixture is chemically inert and has a low viscosity at cryogenic temperatures. The heat exchanger is cooled with liquid nitrogen and has a maximum heat exchange rate of 5.9 kW. A 3.3-kW heating device permits fine temperature adjustments. All parts of the cryogenic system are operated with a temperature control and safety interlock subsystem.

Temperature Regulation

The temperature regulator is a switching mode controller. Absolute temperature is sensed at the wall of the inner vessel by a precision platinum resistance element. A second input for the comparator is derived from the temperature fluctuations found at the discharge end of the heat exchanger. Both signals are electronically used to control the liquid nitrogen supply to the heat exchanger. Several temperature sensors distributed over the entire vessel monitor the temperature distribution. A uniformity and constancy of temperature within 0.3°C is easily maintained except at the end plates, where, due to the poorer heat transfer across the flanges, temperatures a few degrees higher are observed. A number of safety devices are integrated in the control system because of the potential fire hazard posed by the combustible coolant mixture. There are interlocks for excessive temperature of either heaters or coolant, for lack of flow, and for insufficient insulating vacuum. In addition there is a provision to limit the cooldown rate to 1°C/min to avoid excessive stress in the cell wall that might lead to weld cracking.

The requirements on liquid nitrogen for a cooldown and for maintaining a constant temperature are determined by the heat capacity of the 550-kg inner vessel and the cryogenic system and by the radiation and conductive heat transfer. Cooling from room temperature to 200 K requires approximately 600 liters of liquid nitrogen and then 30 liters per hour are needed to maintain this temperature.

Optical System

Modified White Cell Design

The design of the multiple reflection mirror system is based on the concept originally proposed by White.[8] A number of modifications were conceived, however, to meet the design objective of a total path length exceeding 2000 m, while the physical length of the dewar was limited to 11 m by the available laboratory space. Figure 3 shows the mirror arrangement adopted, set for twenty-two passes. Besides the basic set of three concave mirrors A, B, and C, there is a corner mirror assembly D added. This makes it possible to display four rows of images on the surface of mirror A. Compared to the original White design, only one fourth of the mirror width is needed to nest a given number of intermediate images without overlapping. In our case, this number is as large as 124 and the described modification has two significant advantages: first, the amount of astigmatic image distortion is decreased by a factor of 16 (as will be shown in subsequent discussion), and second, the dimensions of mirror A can be held comparable with those of mirrors B and C so that all parts can be cut from one mirror blank, the optimum way to ensure the same radius of curvature for all components of the system.

CerVit-101 (Owens-Illinois, Inc.) was selected as a mirror substrate. This material has an extremely small coefficient of thermal expansion over a wide temperature range ($\alpha < 1 \times 10^{-7}$/°C, −80°C to +125°C), and it can be polished to a high-quality surface finish.[9] Cutting and polishing of the 61-cm

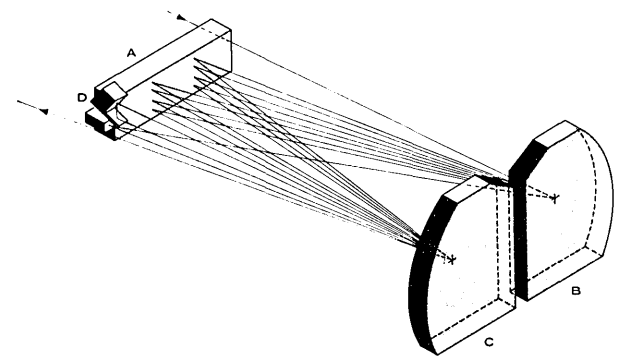

Fig. 3. Four-row multiple reflection system, set for twenty-two passes.

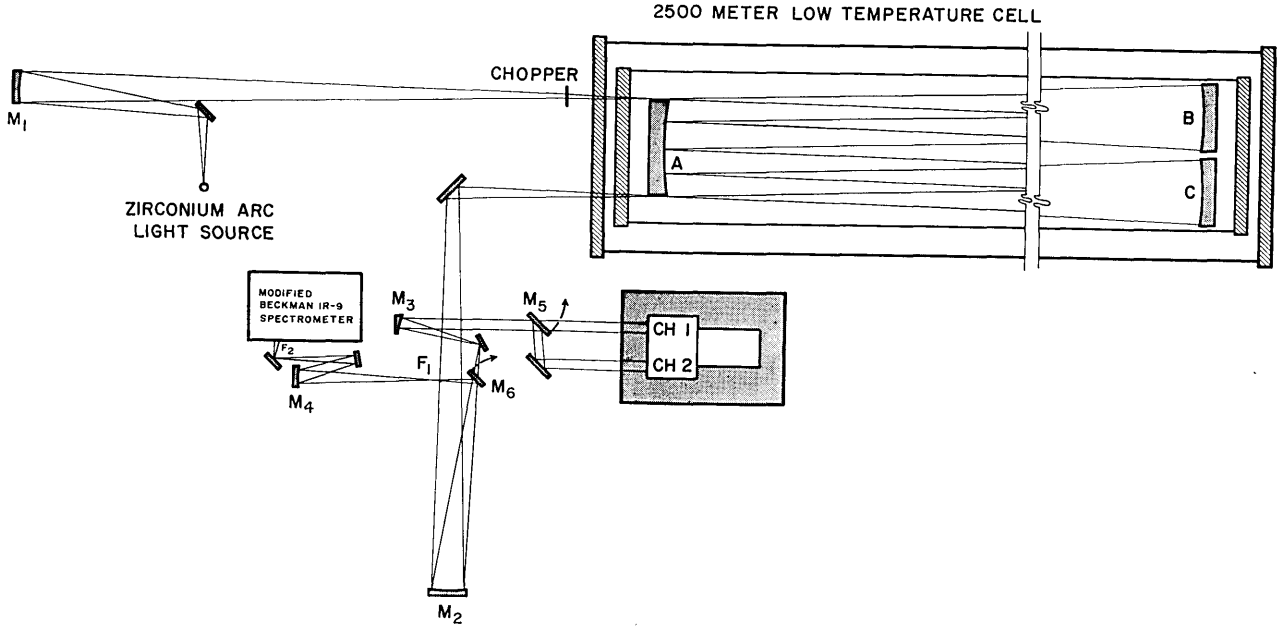

Fig. 4. Optical diagram of the low-temperature multiple-pass cell with entrance and exit optics included. M_1, M_2, and M_4 are spherical mirrors and M_3 is an off-axis paraboloidal mirror. A, B, and C are the spherical mirrors of the multiple-reflection optics; the corner mirror assembly D is omitted. *CH 1* and *CH 2* indicate the options to use the Mariner infrared spectrometer either in channel 1 (4–14.5 μ) or in channel 2 (1.9–6 μ).

mirror blank were performed by Tinsley Laboratories in Berkeley. The optical specifications are 1000.76-cm radius of curvature with a maximum surface departure of $<1\lambda$, $\lambda = 5461$ Å.

Mirrors B and C are mounted so that their centers of curvature fall on the surface of A. As shown in Fig. 4, an external spherical mirror M_1 forms a magnified ($\times 3.5$) image of the point source of a 300-W zirconium-arc lamp[10,11] just off the lateral edge of mirror A. The $f/31$ optical beam diverges to fill mirror B, which is focused so that its center of curvature is at the center of mirror A. The adjustment of A is such that the center of curvature is located on the center line between mirrors C and B. This causes all light emerging from B to be reflected to fill mirror C. Now the rotation of C around its vertical axis determines how many columns of images are displayed on A. A single column gives six passes, hence a minimum path length of 60 m, and each additional column of four images adds eight passes, or 80 m. The maximum path length we have used, 2540 m, is limited by the tolerable noise level due to building vibrations. With improved damping precautions, the optical system would permit a considerably longer maximum path.

Corner Mirror Assembly and Exit Optics

The function of the corner mirror assembly can be understood by inspection of Fig. 3. After completion of the middle two rows of images on A, the optical beam hits the lower, plane mirror of D and an image is formed halfway between the lower and the upper mirror. The upper part of D is also a spherical mirror cut from the original 61-cm mirror blank. This returns an almost vignetting-free reflection of the beam to fill C and to start again a multiple reflection series with a vertically displaced beam. This way a third and fourth row of images is formed on A, exactly in line with and above and below the already existing images of the first and second row. Finally, an exit beam emerges underneath the tab of mirror A.

The exit image is demagnified ($\times 1/3.5$) by the external spherical mirror M_2 (see Fig. 4) to match the f/number of the Beckman spectrometer. Alternatively, by flipping mirror M_6, the optical beam goes to the off-axis paraboloidal mirror M_3 and enters as a parallel beam the telescope system of a Mariner Mars IRS spectrometer,[1] mounted inside a suitable environmental chamber. Depending on the position of M_5, the spectrometer is operated either in the far ir channel 1 (4–14.5 μ) or the near ir channel 2 (1.9–6 μ).

The CsI entrance and exit windows are sealed into SS304 flanges with an epoxy resin (Stycast 2850GT, Emerson and Cuming, Inc.). This resin gives reliable seals even at cryogenic temperatures. To avoid excessive thermal shocks, the windows are mounted on thin-wall SS304 skirts which slow down the heat transfer significantly.

Focusing

Mirrors A, B, and C of the multiple reflection system can be adjusted externally to change the number of reflections and to correct for defocusing as the temperature of the sample compartment is changed. The mirrors are mounted in a rectangular three-point con-

figuration in SS304 mounts. Each mirror holder is spring-loaded and can be moved around a vertical and a horizontal axis by means of two micrometer screws attached to the mounting frame. These micrometer screws are actuated through the end plates of the inner vessel by means of bellows-sealed rotary feedthroughs that penetrate the vacuum wall of the outer vessel. In addition there is capability provided for adjustment of the distance between mirror A and mirrors B and C. Mirror holder A is mounted on a frame constructed as a sliding carriage that rides with Teflon supports on SS304 rods (see Fig. 5). The carriage can be moved back and forth by turning a micrometer screw through two bellows-sealed rotary feedthroughs loosely coupled (for low heat transfer) between the inner and outer chamber walls. This provision is essential, since the cell contracts up to 4 cm in length over the design temperature range. Without correction, this much contraction would cause severe misalignment of the optics and rapidly increasing sizes of successive images. The SS304 micrometer screws are nickel-plated and dry-lubricated with MoS_2 to ensure good high-vacuum and low-temperature performance. Each frame of the mirror mountings is attached to three tabs inside the vessel with one point fixed and the other two sliding freely to allow for differential thermal expansion of the aluminum tank and the SS304 mounting frames. Properly placed Teflon supports and clamps guarantee a strain-free mounting of the mirrors in the holders.

The mount of the corner mirror assembly is made of Invar steel, and it is bolted to the holder of mirror A. The spherical upper part is adjustable but it need not be corrected with varying temperatures due to the exceedingly small thermal expansion of Invar steel and the mirror substrate. Necessary corrections of the adjustment of mirror A do not affect the corner mirror alignment. Figure 5 shows the cage assembly that supports mirrors A and D.

In actual use of the cell, the number of traversals is determined by counting the number of images displayed on A. Mirror A is viewed with a telescope through a viewing port at the opposite end. When the path length exceeds 2000 m, the third- and fourth-row images are no longer visible. This, however, does not prevent the adjustment procedure, since all images in the first and second rows are clearly visible, and the reproducibility, with changing path length, of the vertical columns guarantees the correct arrangement of the third and fourth rows of images.

Mirror Surfaces

All mirrors have an evaporated gold surface deposited in our laboratory under ultra-high vacuum conditions to achieve the highest possible reflectivity in the wavelength range of interest.[12] High-purity gold (99.999%, K & K Laboratories) was evaporated from a molybdenum boat with a rate of about 0.065 g/sec. An oil-free vacuum in the 10^{-9}–10^{-10} Torr range was maintained during the deposition with a 200 liter/sec ion pump system (Ultek–Perkin-Elmer, RCS). The reflectance of the coatings was measured on small control mirrors coated at the same time. These control mirrors could be incorporated in a ir laser reflectometer that operates at 3.39 μ and that permits measurements of reflectances above 99% to an accuracy of $\pm 0.1\%$.[13] Reflectance values of 99.1–99.3% were found for all coatings. Due to the poorer surface quality of the control mirrors, these values are undoubtedly below the reflectance obtained for mirrors A, B, and C. This is a very significant improvement over the 98.4% reflectance that has been obtainable with gold coatings prepared under normal vacuum conditions.[14] For example, at 99.4% reflectance and with 250 reflections, the maximum energy transmission is 22%, a factor of 12 larger than obtainable with 98.4% reflectance.

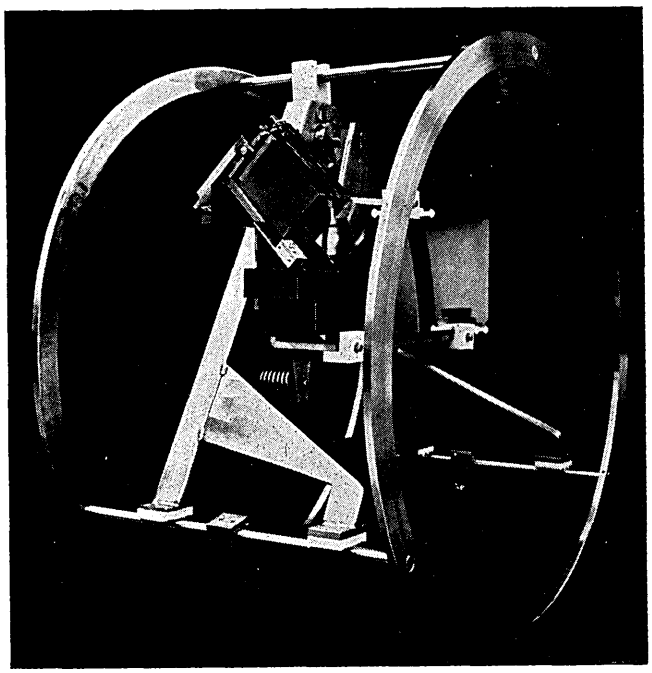

Fig. 5. Sliding carriage for mirror holders for mirrors A and D (mirror D is shown in place).

Astigmatism

In a multiple-reflection system, astigmatism can limit the maximum attainable number of passes even more than reflectivity. This aberration causes an increase of the size of each successive image and eventually image overlapping. For the optical system described here the astigmatic increase Δl of the image diameter can be estimated as follows (see Appendix for derivation):

$$\Delta l = \frac{d^2}{rf}\left[\frac{1}{4} + \frac{1}{j^2}\sum_{K=1}^{K=j}(j-K)^2\right],$$

where f = f/number of the multiple reflection system,
d = width of mirror A,
r = radius of curvature of mirrors A, B, and C,
j = number of columns of images on A = $(N+2)/8$,
N = number of passes,
Δl = increase of image diameter.

With an image diameter of 1 cm (this is the ×3.5 magnified image of a 300-W zirconium-arc light source), $f = 31$, $d = 37$ cm, $r = 1000$ cm, and $N = 198$, there is an astigmatic diameter increase of $\Delta l = 0.36$ cm. This estimate, which is a tolerable amount of distortion, was checked experimentally. After 198 passes an exit image that showed no noticeable distortion could still be observed on a screen located at focal position F_1 (Fig. 4.)

In order to decrease the stray light level of the cell, entrance and exit stops are attached to the holder for mirror A. They are located within 6 cm of the focal plane and the stop diameter matches the beam diameter closely. The amount of stray light was estimated by displacing the exit beam slightly so that only non-focused stray light could emerge through the exit stop. With a path length of 1980 m the stray light detected was less than 1% at any wavelength in the spectral range 2–14 μ.

Applications

The cell has been used to determine the curve of growth for the 2-μ triplet of carbon dioxide at room temperature[15] and at 200 K.[16] Similar measurements were performed on a number of other gases to establish upper limits on possible minor constituents of the Martian planetary atmosphere.[17] In these investigations a maximum pathlength of 2540 m was achieved routinely. Disturbances of the optical system by building vibrations limit at present the maximum path to this length. More effective means of damping, however, would permit use of this multiple reflection cell at path lengths up to 3–4 km, now probably limited by reflectance losses.

We wish to thank E. Valenzuela and K. C. Herr for placing the 20-m low-temperature cell and the experience they gained with it at our disposal. We appreciated the considerable help we received from J. M. McAfee and R. E. Challey in the ultra-high vacuum coating of the mirrors and in measuring their reflectivities. Finally, we wish to acknowledge support from the National Aeronautics and Space Administration for the construction of this cell and the Deutsche Forschungsgemeinschaft for fellowship support for one of us (D. H.).

Appendix

The amount of astigmatic image distortion in a four-row multiple reflection system of the type described here can be estimated from the well-known formulas for the location of the tangential and sagittal focal lines of an astigmatic image

$$(1/a) + (1/t) = [2/(r\cos\varphi)] \quad \text{and}$$

$$(1/a) + (1/s) = [(2\cos\varphi)/r],$$

where φ = angle of incidence,
a = object distance,
t = distance of tangential focal line,
s = distance of sagittal focal line,
r = radius of curvature.

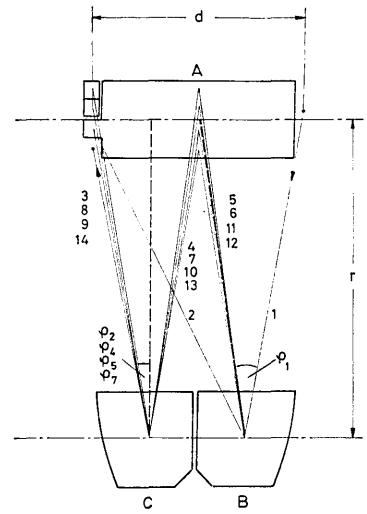

Fig. 6. Optical path in a four-row multiple-reflection system pertaining to the derivation of the astigmatic image distortion. The optical axes of mirrors B and C are marked by dashed lines. Successive passes are numbered from 1 to 14. Angle φ_1 belongs to passes 1 and 2, angle φ_2 to passes 3 and 4, etc. For the chosen adjustment of fourteen passes, angles φ_3 and φ_6 are zero.

We obtain for the distance $s - t$

$$s - t = (2ra^2\sin^2\varphi)/[(4a^2 + r^2)\cos\varphi - 2ar(1 + \cos^2\varphi)],$$

and since, to a good approximation, $r = a$, $\cos\varphi = 1$, and $\sin\varphi = \varphi$, this reduces to

$$s - t = 2r\varphi^2 \equiv \Delta S.$$

For successive reflections, the off-axis angle φ changes, and since the contributions for different φ to the total ΔS can be assumed to be additive, we have[18]

$$\Delta S_{\text{total}} = 2r\Sigma\varphi_i^2.$$

Of course, $\Sigma\varphi_i^2$ depends on the adjustment of the mirrors. Consider, for example, the path of a central ray for fourteen passes, which places a column of four images at the center of mirror A (see Fig. 6). There are seven angles of incidence to consider, φ_1 to φ_7, and with $r \gg d$, we obtain

$$\varphi_1 = d/(2r), \qquad \varphi_2 = \varphi_4 = \varphi_5 = \varphi_7 = [d - (d/2)]/2r,$$

$$\varphi_3 = \varphi_6 = 0.$$

Therefore, we find for ΔS_{total}

$$\Delta S_{\text{total}} = 2r\left[\frac{d^2}{4r^2} + 4\cdot\frac{d^2}{4r^2}\,(\tfrac{1}{2})^2\right].$$

The number of passes increases as the center of curvature of C is moved closer to that of mirror B (which is always located at the center of mirror A). Columns of four images will be displayed on the surface of A at spacings d/j, where d is the width of mirror A and j is the number of columns of images, which runs from 1 to 32, depending on the adjustment of the system for 60–2540 m. In terms of j, the total pathlength L is given by $L = (8j - 2)\,10$. Now, the generalization of the

expression for ΔS_{total} for N passes [$j = (N+2)/8$] can be shown to be

$$\Delta S_{\text{total}} = \frac{2d^2}{r}\left[\frac{1}{4} + \frac{1}{j^2}\sum_{K=1}^{K=j}(j-K)^2\right].$$

Finally, we calculate the diameter of the circle of least confusion, which lies halfway between the tangential and sagittal focal planes, and then subtract the diameter of the initial image to find Δl, the distortion due to astigmatism. With the assumption that $r \gg \Delta S_{\text{total}}$ one obtains by a straightforward geometrical consideration

$$\Delta l = (\Delta S_{\text{total}})/(2f).$$

In this derivation only the horizontal off-axis angle is considered. The vertical displacement of the beam is always so small that the corresponding contributions to the distortion are negligible.

References

1. The ir spectrometers were designed and constructed in the Chemistry Department and the Space Sciences Laboratory at the University of California, Berkeley. This instrument will be described in detail in a later publication. Mariners VI and VII were NASA missions managed by the Jet Propulsion Laboratory and directed by Project Manager H. M. Schurmeier.
2. G. Herzberg, Astrophys. J. **115**, 337 (1952).
3. A. Watanabe and H. L. Welsh, Can. J. Phys. **45**, 820 (1965).
4. R. P. Blickensderfer, G. E. Ewing, and R. Leonard, Appl. Opt. **7**, 2214 (1968).
5. D. E. Burch, D. A. Gryvnak, and R. R. Patty, J. Opt. Soc. Am. **57**, 885 (1967).
6. A multiple-reflection cell with a 20-m optical path which would operate at 77 K was constructed in our laboratory by E. Valenzuela and K. C. Herr, providing experience valuable in our design of the cell described here.
7. A. R. W. McKeller, N. Rich, and V. Soots, Appl. Opt. **9**, 222 (1970).
8. J. U. White, J. Opt. Soc. Am. **32**, 285 (1942).
9. R. E. Cox, Sky and Telescope **32**, 159 (1966).
10. W. D. Buckingham and C. R. Deibert, J. Opt. Soc. Am. **36**, 245 (1946).
11. A commercially available arc (Sylvania) was modified by adding a water-cooled envelope fitted with a salt window. After modification, the envelope was reevacuated and filled with argon to a pressure of 300 Torr.
12. J. M. Bennett and E. J. Ashley, Appl. Opt. **4**, 221 (1965).
13. This reflectometer was constructed by D. Horn and J. M. McAfee using components from the 20-m multiple-reflection cell mentioned in Ref. 6.
14. G. Hass, J. Opt. Soc. Am. **45**, 945 (1955).
15. K. C. Herr, D. Horn, J. M. McAfee, and G. C. Pimentel, Astron. J. **75**, 883 (1970).
16. G. C. Pimentel *et al.*, to be published.
17. G. C. Pimentel *et al.*, to be published.
18. T. R. Reesor, J. Opt. Soc. Am. **41**, 1059L (1951).

OSA Instructions for Post-Deadline Papers

The Executive Committee of the Board of Directors, at its meeting on 9 December 1970, instituted a new policy toward presentation of post-deadline papers at the semiannual meetings of the Society. In order to give participants at the meetings an opportunity to hear new and significant material in rapidly advancing areas of optics, authors will be provided with the opportunity to present results that have been obtained after the normal deadline for contributed papers. The regulations that govern the submission of post-deadline papers follow:

(1) In order to be considered for the post-deadline session(s) an author must submit a 1000-word summary in addition to the information required on the standard abstract form. The 1000-word abstract will be used in selecting papers to be accepted. The 200-word abstracts of accepted papers will be published in the Journal of the Optical Society of America.

(2) Post-deadline papers are to be submitted to the Executive Director, Optical Society of America, 2100 Pennsylvania Avenue, N.W., Washington, D.C. 20037. Only those received by the Thursday preceding an OSA meeting can be duplicated and distributed in time for the program committee meeting.

(3) The program committee for the selection of post-deadline papers consists of the Technical Council, the Executive Director, and any others designated by the chairman of the Technical Council. This group will meet before the first full day of the OSA meeting. The chairman of the Technical Council, or someone designated by him, will preside.

(4) Only post-deadline papers judged by the appropriate members of the program committee to be truly excellent and compelling in their timeliness will be accepted.

(5) The accepted post-deadline papers will be placed at the end of related sessions of contributed papers, if possible, or in a separate session if necessary. The number of papers accepted will be governed by the time available as well as by the requirements of Regulation (4).

(6) Multiple papers by the same author will be handled in a manner consistent with OSA policy. Accepted post-deadline papers will have priority over multiple papers by the same author that are scheduled in the same session.

(7) After post-deadline papers have been selected, a schedule will be printed and made available to the attendees early in the meeting. Copies of the 200-word abstracts will also be available.

(8) The 200-word abstracts will be printed in the Journal in due course. They will not appear with the regular program but at a later date as the printing schedule permits.

(9) The selection and scheduling of post-deadline papers will be done with the interests of the attendees given principal consideration.